



Kenneth L. Blaedel, Center Leader

The mission of the Center for Precision Engineering at Lawrence Livermore National Laboratory (LLNL) is to ensure that programs have available an adequate base of high-precision design and manufacturing technology, not necessarily resident at LLNL, to help solve their critical future problems.

Our specific goals are 1) to develop an understanding of fundamental fabrication processes and the models that reflect that understanding; 2) to advance methods of the design of machinery that incorporate those fabrication processes; and 3) to maintain continuing relationships among our colleagues in industry, government and academia that promote our collective capabilities in precision engineering.

In support of these goals, three projects are reported here that bring either higher precision or lower cost-of-precision to the manufacturing challenges that we face over the next few years.

The first project, "Micro-Drilling of Beryllium Capsules," has seen significant advance. Last year's conclusion was that the evolutionary changes in commercial capability could not be expected to laser-drill holes small enough and precise enough for future National Ignition Facility (NIF) capsules. This year's result, which included holes made with a femto-second laser, holds promise for being able to do so.

The second report, "A Spatial-Frequency-Domain Approach to Designing Precision Machine Tools," presents a new view of how we can design machine tools and instruments to make or measure parts that are specified in terms of the spatial frequency content of the residual errors of the part surface.

This represents an improvement in our ability and a reduction in cost to design manufacturing machines in comparison to using an "error budget," a design tool that saw significant development in the early 1980s, and has been in active use since then.

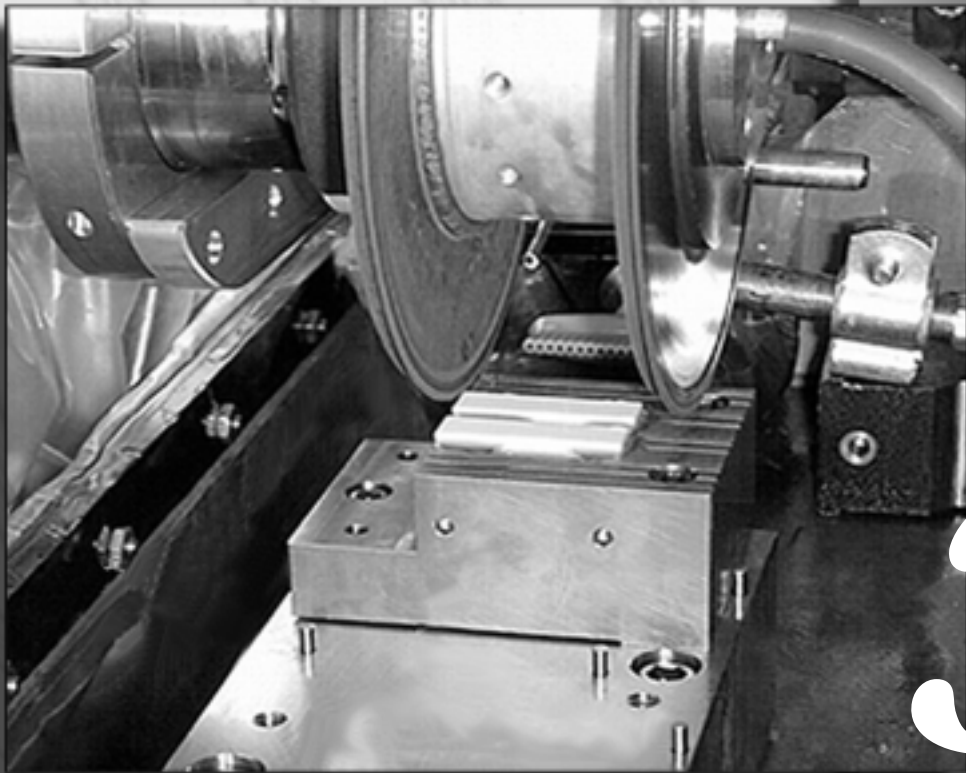
The third project, "Precision Grinding of Microfeatures in Brittle Materials," demonstrates our ability to develop high-precision manufacturing processes and then convey them to commercial industry, which can then supply that technology for high production.

In addition to conducting the three projects above, the Center for Precision Engineering holds membership in two academic consortia, allowing us insight into broader areas of precision engineering that we cannot pursue ourselves.

Looking to the future of precision engineering at LLNL, we have drawn two conclusions. First, conducting the business of LLNL will require machinery capable of material removal, deposition, and metrology to produce components and assemblies to atomic-level dimensional tolerances. Second, significantly reducing the cost of precision for component manufacture and for assembly of precision products will actually enable many LLNL projects. It is in projects such as NIF that the expenses of precision manufacturing can defeat big physics.

With the focus of this year's projects on creating high-precision processes and instruments at acceptable cost, we think the Center for Precision Engineering has materially contributed to LLNL's ability to field small- and large-scale science.

Center for Precision Engineering



3

3. Center for Precision Engineering

Overview

Kenneth L. Blaedel, Center Leader

Micro-Drilling of ICF Capsules

Steven A. Jensen and Brent C. Stuart3-1

A Spatial-Frequency-Domain Approach to Designing Precision Machine Tools

Debra A. Krulewich3-3

Precision Grinding of Brittle Materials

Mark A. Piscotty, Kenneth L. Blaedel, Pete J. Davis, and Pete C. Dupuy.....3-9

icro-Drilling of ICF Capsules

Steven A. Jensen

*Manufacturing and Materials Engineering Division
Mechanical Engineering*

Brent C. Stuart

*Laser Science and Technology
Laser Programs*

Further studies are reported on micro-drilling of holes in fusion capsules. This update outlines the preliminary efforts using short-pulse (≈ 100 fs) lasers to potentially drill holes in the ICF capsules.

Introduction

This report serves as an update to "Micro-Drilling of ICF Capsules."¹ In that report the commercial capabilities of micro-drilling small holes were investigated for limits of precision, quality, and attainable aspect ratios. The motivation behind the investigation was to determine the feasibility of drilling small holes in the National Ignition Facility (NIF) fusion capsules, suitable for filling with the intended fuel mixture.

The report concluded that although the micro-drilling of holes in the fusion capsules is feasible, the commercial sector currently cannot produce these holes. SEM photos of commercially drilled holes showed an excessive amount of thermal damage (that is, dross, re-melt, and thermal cracking) due to laser pulse lengths of relatively long durations (nanosecond and longer). Melt-expulsion, and not evaporative ablation, largely dominates the mechanism behind commercially drilled holes.

Furthermore, most commercial companies are not equipped with the appropriate lenses and laser set-up to drill holes smaller than $5\text{ }\mu\text{m}$ because current demand is limited. It was speculated in the FY-97 report,¹ based solely on published data, that lasers with pulse lengths in the femtosecond to 0.1 ps range could eliminate much of the thermal damage and potentially produce small enough holes to meet stringent NIF requirements.

This update outlines the preliminary efforts using short-pulse (≈ 100 fs) lasers to potentially drill holes in the ICF capsules.

Progress

The ICF capsules will be made of doped beryllium (Be) having an ablator shell thickness between 100 and $150\text{ }\mu\text{m}$. Therefore, the goal of the preliminary studies was to drill $5\text{-}\mu\text{m}$ or smaller holes through $125\text{-}\mu\text{m}$ -thick Be foil. In our experiments the Be foil was mounted on a xyz-translation stage in a vacuum chamber pumped down to 25 mTorr . The experiments were performed using a 1-kHz , 120-fs , Ti:Sapphire short-pulse laser system. Numerous combinations of spatial filtering, focus lens, f-number, and wavelength were tried and the best focal spot obtained was $5\text{-}\mu\text{m}$ $1/e^2$ diameter (where spot size is defined as the distance at which the Gaussian beam intensity has dropped to $1/e^2 = 0.135$ times its peak value).

To achieve this, the laser output was spatially filtered, frequency doubled to 413-nm , spatially filtered again, and then focused with a 25-mm focal length GRIN lens (LightPath) at approximately f-number = 5 . Both the quality of the BBO doubling crystal ($\lambda/2$ surface) and the choice of focusing lens leave room for reducing the focal spot size.

SEM images, after ultra-sonic cleaning, of one of the smallest holes obtained are shown in **Fig. 1**. The entrance diameter is approximately $6.5\text{ }\mu\text{m}$, while the exit diameter is approximately $3\text{ }\mu\text{m}$. This gives a taper angle of approximately 1.6° which is significantly better than the 4 to 12° that was seen in commercially drilled holes. This hole was drilled with approximately $1.8\text{-}\mu\text{J}$ pulses (18J/cm^2) at 1 kHz in 12 s .

These preliminary studies are encouraging. The diameter of the heat-affected zone is much smaller than commercially drilled holes. There were no visible signs of thermal cracking and the re-melt around the walls was minimal. Furthermore, the taper angle associated with the hole is much smaller than has been seen in commercially drilled holes. It is speculated that the focal spot size can be further reduced to approximately 2 μm in diameter by using a smaller f-number and possibly third harmonics. With some fine-tuning of parameter settings these holes could potentially meet NIF standards.

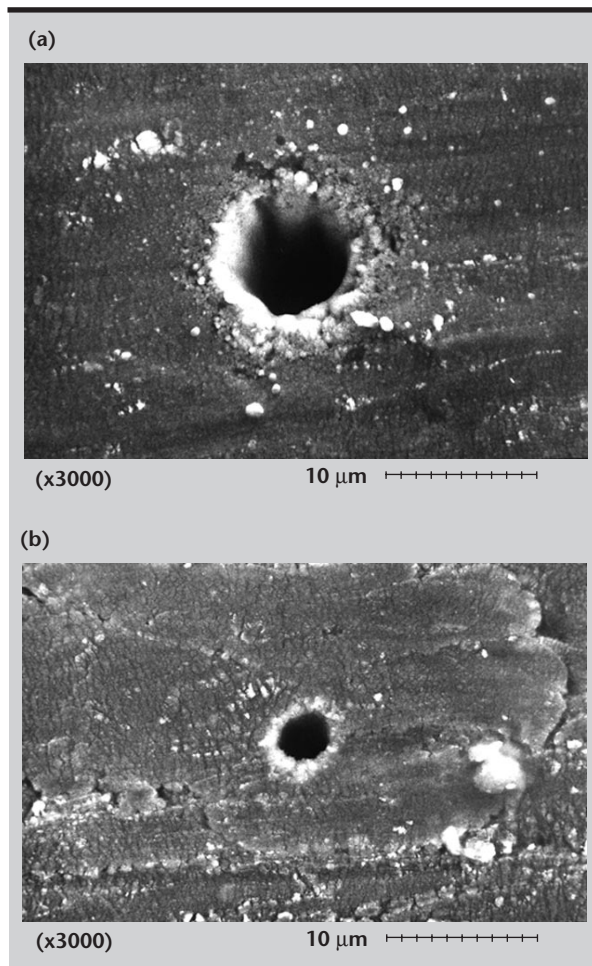


Figure 1. SEM images of smallest holes obtained: a) entrance hole; and b) exit hole.

Having performed these preliminary studies and prior to further studies, the question of “how small is small enough” remains to be answered. Initial indications suggested that entrance hole diameters on the order of 1 to 2 μm in diameter would be small enough. However, studies need to be performed which ultimately back up these initial estimates and quantify the largest allowable capsule perturbation that would affect the hydrodynamic stability and hinder a symmetrical implosion. Whether this work is done experimentally or through simulation, it is necessary to validate the continued efforts of reducing and refining the micro-drilled hole.

Assuming that a 1- to 2- μm hole would be sufficiently small, there are still issues that must be resolved if this approach to capsule filling is to succeed. The hole will need to be sealed shut once the capsule is filled with the intended fuel mixture of deuterium-tritium (DT). The sealing process, like the drilling process, will have to minimally affect the integrity and surface quality of the capsule. Work needs to be done to determine the extent and size of the area around the hole affected by the sealing process. Ideally it would be desirable to use the same laser set-up to seal the holes as was used to drill them. This might be accomplished by reducing the intensity of the beam and/or using longer pulse durations to sinter the hole shut. The feasibility of this approach also remains to be studied.

In addition to the sealing process, a micro-polishing process may be necessary to smooth over ablator shell perturbations due to the sealing process. This would also help to ensure a surface roughness that meets specifications. Currently, the specification for surface roughness is on the order of 10 nm rms or less, and efforts thus far have not produced capsules with a surface roughness less than 50 nm rms. Micro-polishing of the capsules needs to be studied, since this process may be needed even if diffusion filling is adopted as the approach to capsule filling.

Reference

1. Jensen, S. A., “Micro-Drilling of ICF Capsules,” *Engineering Research, Development and Technology*, Lawrence Livermore National Laboratory, Livermore, California (UCRL-ID-129204).

A Spatial-Frequency-Domain Approach to Designing Precision Machine Tools

Debra A. Krulewich

*Manufacturing and Materials Engineering Division
Mechanical Engineering*

The aim of this project is to develop a methodology to design machines used to manufacture parts with spatial-frequency-based specifications, thus reducing risk while maintaining accuracy. Using an error budget, we are able to minimize risk during the design stage by ensuring that the machine will produce components that meet specifications before the machine is actually built. Minimizing the risk while maintaining accuracy is a key manufacturing goal for programs that cannot tolerate yield factors less than 100%, such as the nuclear weapons program. Current error budgeting procedure provides no formal mechanism for designing machines that can produce parts with spatial-frequency-based specifications. However, recent specifications for advanced optical and weapons systems are being posed in terms of the continuous spatial frequency spectrum of the surface errors on the machined part. Based on these requirements, it is no longer acceptable to specify tolerances in terms of a single number that spans all temporal and spatial frequencies. During this project, we will develop a new error budgeting methodology to aid in the design of new machines used to manufacture parts with spatial-frequency-based specifications.

Introduction

Increased precision in manufacturing is being demanded by Lawrence Livermore National Laboratory (LLNL) Programs in areas ranging from NIF optics manufacturing and ICF target positioning, to the production and alignment of optics for EUV lithography. Other LLNL areas that drive unique requirements for precision include the machining of diffractive optical systems, the fabrication of ICF targets, and the assembly/packaging of fiber optical systems.

The precision-to-cost ratio is another metric that relates to a wide variety of industrial mechanical systems, such as automotive engine components, but has a special significance at LLNL where an increased interest in tighter tolerances is matched by the need to lower program costs. Minimizing technical risk while maintaining precision is a complementary issue that defines manufacturing goals for programs that cannot tolerate yield factors less than 100%, such as in fabricating components for the nuclear weapons program.

This project presents an opportunity to significantly improve the foundation that underlies our precision engineering expertise: the process of formulating an error budget for a manufacturing, positioning, or measurement system. Error budgets

provide the formalism whereby we account for all sources of uncertainty in a process, and sum them to arrive at a net prediction of how “precisely” a manufactured component can meet a target specification. The error budgeting process drives decisions regarding the conceptual design of the system and choice of components and subsystems, and enables a rationale for balancing precision (performance), cost, and risk.

The principles of designing precision instruments for meeting challenging tolerance requirements have a rich history.¹ Likewise, the methodologies for analyzing the errors in experimental data and performing differential sensitivity analyses are well-documented.^{2,3} Yet the first clear formalization of error budgeting applied to precision engineering appears to originate in the analysis by R. Donaldson during the design of the Large Optics Diamond Turning Machine at Lawrence Livermore National Laboratory (LLNL).⁴ Donaldson’s formalism is referenced in current textbooks⁵ and is the basis for subsequent machine designs at LLNL.⁶

Figure 1 shows flowcharts for both the conventional and the new error budget procedure and how they differ. The upper portion of **Fig. 1** shows Donaldson’s flowchart illustrating the mapping of error sources onto part geometry.

The first step of the conventional error budget is to identify the physical influences that generate the dimensional errors that propagate through the machine tool. These include effects such as thermal gradients and temperature variability, bearing noise, fluid turbulence in cooling passages, and way non-straightness.

The second step is to determine how this source couples to the machine. A coupling mechanism converts these physical influences into a displacement that has a direct influence on machine performance. An example of a coupling mechanism is the thermal expansion that may transform a time-varying heat source in the vicinity of the machine into a machine way distortion. These displacements represent dimensional changes in the system. A single peak-to-valley number is usually used to quantify the dimensional changes, not differentiating between the spatial frequency content of the error.

The next step is to sum all the contributing errors using an appropriate combinatorial algorithm. Literature suggests a variety of combinatorial algorithms.⁷

The last step in the error budgeting procedure is to transform these errors into the workpiece coordinate system. To convert these machine displacements into the errors that would reside on the workpiece surface in the directions of interest, we must consider the tool path (feed rates and spindle speeds, for example).

The output from this procedure is a single number predicting the net error that would result on a machined workpiece. We would then compare this number to the part specifications. If the prediction meets target specifications, we would accept the machine design under evaluation. If the prediction does not meet specifications, we would evaluate methods to improve this design by observing which

sources are the dominating contributing errors. In this way we can evaluate the cost vs accuracy of different candidate designs.

If improvements could be made to an existing design, we would make those changes to the error budget and reevaluate the net error. If the modifications were not practical, we would then consider an entirely new design, or possibly reevaluate the specifications.

Progress

The lower portion of **Fig. 1** shows the new error budget approach. The first two steps, identifying the sources and how they couple to the machine, are identical and are explained in the previous section. However, the new approach differs in the next step, where the elemental errors are converted into the frequency domain. The next step is to combine the errors in the frequency domain. The combinatorial rule is a completely new algorithm with a statistical foundation. These steps are explained below.

Figure 2 displays a block diagram of the machining process. During cutting, an instantaneous amount of material is removed, which creates forces. The ratio between the cutting force and amount of material removed is the material removal transfer function. These cutting forces combine with forces induced by the machine errors. The machine structure responds with displacements that ultimately result in errors on the machined part.

The conventional error budgeting approach does not consider the dynamics of the material removal transfer function. In other words, the conventional approach assumes that the forces are directly proportional to the amount of material removed, so the cutting process doesn't damp or amplify the error sources at certain frequencies. Our proposed

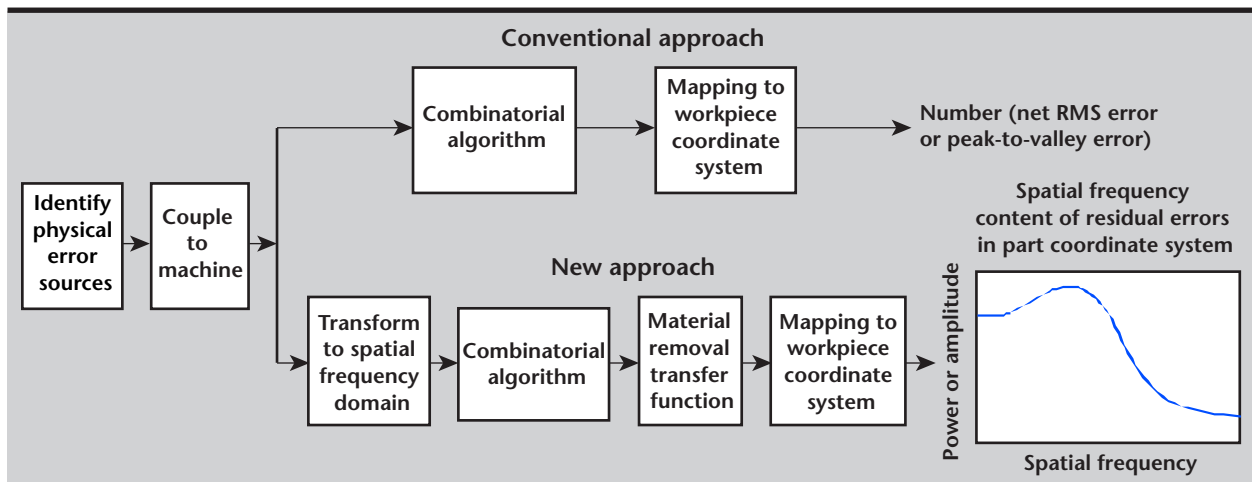


Figure 1. Flowcharts for both the conventional and the new error budget.

approach considers the dynamics of the material removal transfer function. The last step is to transform the errors into the part coordinate system. The output from this process is the continuous spectrum of errors at all spatial frequencies on the part. Each component in this block diagram is described below.

We are performing experimentation and validation of each step in the error budgeting procedure on a T-based lathe. Test results are also discussed in the following sections.

Transforming Errors into Spatial-Frequency Domain

Conventionally, a single peak-to-valley number is used to quantify the dimensional changes, not identifying the spatial frequency content of the error. This new approach requires us to determine the full frequency spectrum of the errors. To do this, we must relate the error characteristics to physical properties of the system. Forces generate the dimensional errors. The machine structure responds to these forces due to the compliance of the machine, as shown in the block diagram of **Fig. 2**.

Often the forces are related to physical properties of the machine, such as the cycling of the rolling elements in bearing systems or the number of poles in a motor. However, when these forces are at or near the machine resonances, the displacements caused by these forces are amplified.

While the frequency content of the error forces is often fixed in the spatial-frequency domain, the machine resonance is fixed in the temporal-frequency domain. The spatial frequency is converted to the temporal frequency by multiplying the spatial frequency by the velocity. While the spatial frequency content of the force error may be independent of velocity, the

spatial frequency content of the displacement error is dependent on velocity.

For example, consider a machine with a resonance at 100 Hz. If the axis velocity is 10 in./min, then 600 cycles/in. is equal to 100 Hz in the temporal-frequency domain and is amplified by the machine resonance. However, if the axis velocity is 100 in./min, then 60 cycles/in. is equal to 100 Hz and is amplified by the machine resonance. Therefore, the spatial-frequency content of the displacement error is dependent on the velocity of the moving components.

We observed this effect when we measured axial and radial error motions of the spindle on our test machine. As expected, the air-bearing spindle is very repeatable with sub-micrometer levels of asynchronous motion. However, the error characteristics drastically change at different spindle speeds. For example, the axial motion at 840 RPM spindle speed has a synchronous error with a dominant lobing of 17, 18 and 19 cycles/revolution, as shown in **Fig. 3**. If the errors were associated with a physical property of the motor such as the number of commutations, we would expect the spatial frequency of the lobing to remain fixed. However, at a spindle speed of 300 RPM, we observed a much higher spatial frequency lobing pattern, as seen in **Fig. 4**.

In general, the spatial frequency of the lobing increases with decreasing spindle speed. However, the temporal frequency of the dominant errors remain in the same region for all spindle speeds, as shown in the plots on the right sides of **Figs. 3** and **4**.

We are investigating the source of the forcing function. It is curious that the forcing function remains almost completely synchronous. Our hypothesis is that the forcing function is due the spindle speed variations about the set point. This will be investigated further during the next fiscal year.

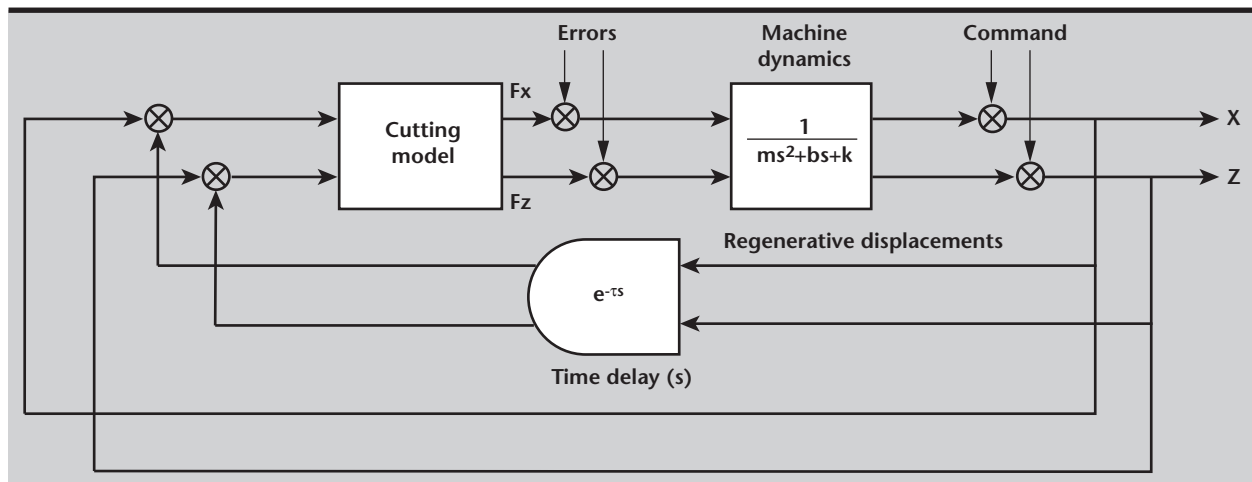


Figure 2. Block diagram of the machining process.

We also observed a similar effect with the straightness errors. The cycling of the balls in the bearing system causes the lower frequency displacement errors. This component is fixed in the spatial-frequency domain and remains constant at different feed rates of the axis. However, the higher frequency displacement errors fell at the machine resonances, which are fixed in the temporal-frequency domain. Therefore, the spatial-frequency spectrum of the displacement errors is dependent on the axis feed rate.

Combinatorial Rule

We have developed a combinatorial rule for the addition of the frequency content of each elemental error. The key to the combinatorial algorithm is to consider the spectrum of each elemental error as the sum of sinusoidal errors at specific frequencies. The addition of two sinusoidal signals at a given frequency results in a sinusoidal signal with the same frequency, but the amplitude can vary anywhere from the direct difference to the sum of

the two amplitudes, depending on the phase shift between the two signals.

We first identify all elemental errors that are correlated, and appropriately sum the amplitudes of these errors. We then consider the phase shift between the remaining elemental errors to be uniformly distributed variables between 0 and 2π . We have analytically shown that the expected value of the square of the net amplitude is equal to the sum of the squares of the amplitudes of each elemental error. This is equivalent to saying that the expected net power spectral density (PSD) is the sum of the elemental PSDs.

Furthermore, we can now determine the probability distribution function of the net error with the use of a Monte Carlo simulation. The 95% confidence limit of the net PSD is approximately three times the mean, and the 99% confidence limit is approximately 4.6 times the mean. This is significantly less than the worst case error. For example, if 25 errors of equal amplitude were summed, the worst case net PSD would be over eight times larger than the 95% confidence

Figure 3. Axial errors at 840 RPM.

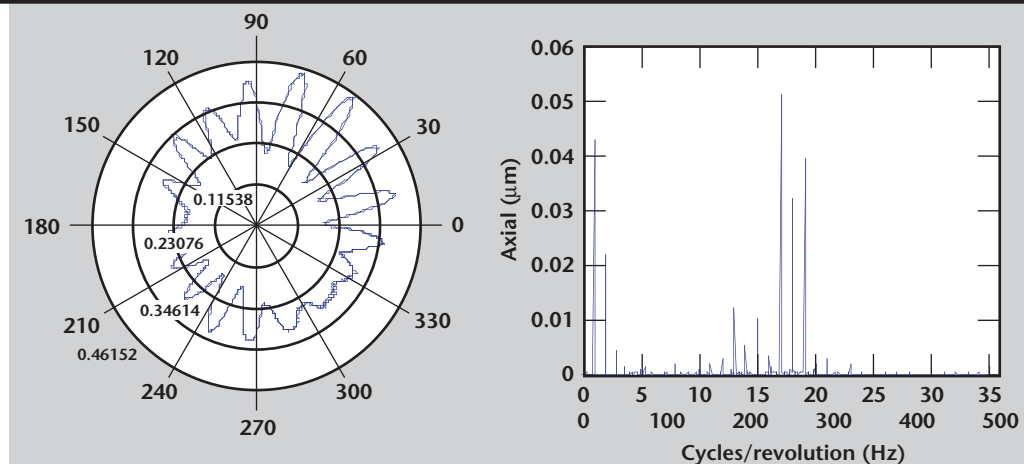
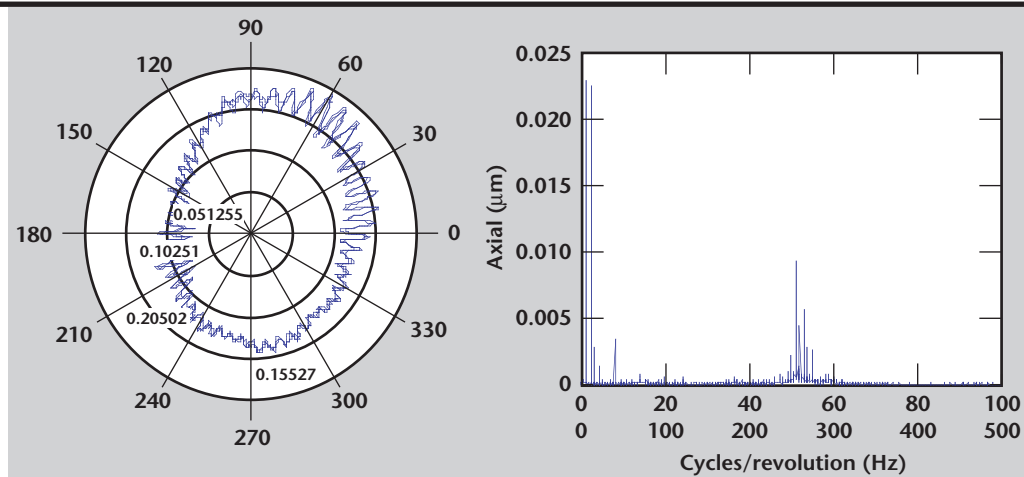


Figure 4. Axial errors at 300 RPM.



limit, and over five times larger than the 99% confidence limit.

Material Removal Transfer Function

The purpose of the material removal transfer function is to convert the motion of the tool in free space to the motion of the tool in the part during the cutting process. This step is necessary because current error characterization procedures measure the error motion of the tool in an open loop sense. The loop is closed when tool is in contact with the part during the cutting process. Differences occur when the loop is closed due to static and dynamic stiffness of the machining process.

The conventional error budgeting procedure assumed that the measured motion of the tool in free space is the same as the motion of the tool in the part during cutting. In other words, it assumes that the transfer function equals one. We have analytically shown that the material removal transfer function equals one under the following assumptions: 1) we have made multiple cutting passes on the part; 2) the material removal transfer function is linear; and 3) the errors can be adequately represented in the frequency domain with negligible random components.

While the first assumption is valid, the second and third assumptions are invalid. However, to a first order approximation, we have experimentally determined that the material removal transfer function is approximately linear around small deviations in the operating point. Furthermore, precision machines often have very repeatable error characteristics, so the third assumption is valid to first order.

Mapping the Errors into the Workpiece Coordinate System

Given the frequency content of the error motion of the tool during cutting, we must take into consideration that the path of the tool and the tool geometry determine the frequency content of the residual surface errors on the workpiece. Typical tools with a round cutting edge impart a nominal surface finish, or scalloping, during turning, even for a process with no errors. Next, we consider the exact path of the tool during the entire cutting procedure to map these errors onto the relevant workpiece coordinate system.

For example, during a facing operation on a diamond turning machine, the part turns while the tool remains stationary. Consider the spatial frequency content of a radial trace across the

workpiece. The turning process can be considered a sampling mechanism. The radial trace is composed of the time domain sampling of the tool motion once every revolution of the part. Once every revolution, the tool falls on the radial trace of interest, leaving behind the signature of the tool as well as any error motions.

The description of the process so far has been in the time domain. However, we are interested in the frequency domain. Sampling in the time domain can be decomposed into a multiplication procedure of the original time-domain signal by a series of impulses. Since multiplication in the frequency domain is equivalent to convolution in the frequency domain, the sampling procedure is converted to the frequency domain by a convolution process. Note that unavoidable aliasing occurs for errors with higher frequency content than the rotational speed of the spindle. Note also that errors at frequencies that are an even multiple of the spindle speed (such as 'synchronous' spindle errors) do not appear on the radial trace due to this aliasing.

The imparting of the tool geometry onto the workpiece can be considered a convolution in the time domain. Conveniently, convolution in the time domain is equivalent to multiplication in the frequency domain. Therefore, the imparting of the tool geometry onto the workpiece in the frequency domain can be considered a filter.

Future Work

Transformation of Errors into Spatial-Frequency Domain

During experimentation and validation, we have been able to measure the contributing errors. However, during the design process, we will not have this luxury. Therefore, we must relate the physical properties of the machine to the general types of errors that are created. For example we discussed the error motions of the spindle. We believe that these errors arise from the fact that the spindle speed is varying, due to the spindle/motor/controller system. During FY-99 we will relate the physical properties of general machine components to the frequency content of errors that are associated with these types of systems.

Material Removal Transfer Function


For simplification we assumed that the material removal transfer function was linear. This is known to be false. During FY-99 we will study the nonlinearities associated with the cutting process and

develop strategies to deal with these nonlinearities in the frequency domain.

Error Budget Procedure

At the end of FY-99 we will deliver an error budgeting procedure to predict the spatial-frequency content of errors on a machined part for a variety of machining conditions. The user will input specifics about the machine components, structure, and control systems along with machining parameters such as spindle speed and axis velocity. Software will perform the appropriate combinatorial algorithm and processing to predict the spatial-frequency content of the errors on the machined surface of the part. With this tool, the user can study the effect of changing machining parameters or system components on the spatial-frequency content of the errors on the machined part. For example, the user will be able to replace the spindle type or axis velocity and observe the effects on the spatial-frequency content of the errors on the machined part.

References

1. Evans, C. (1989), *Precision Engineering: An Evolutionary View*, Cranfield Press, Bedford, UK.
2. Bendat, J. S., and A. G. Piersol (1986), *Random Data: Analysis and Measurement Procedures*, 2nd ed., Wiley-Interscience, New York, New York.
3. Sokolnikoff, I. S., and R. M. Redheffer (1966), *Mathematics of Physics and Modern Engineering*, 2nd ed., McGraw-Hill, San Francisco, California, p. 319.
4. Donaldson, R. R. (1980), "Error Budgets," in *Machine Tool Accuracy*, Vol. 5 of *Technology of Machine Tools: A Survey of the State of the Art by the Machine Tool Task Force*, R. Hocken, ed., Ch. 9.
5. Slocum, A. H. (1992), *Precision Machine Design*, Prentice Hall, Princeton, New Jersey.
6. Thompson, D. C. (1989), "The design of an ultra-precision CNC measuring machine," *39th CIRP General Assembly*, Trondheim, Norway, August 20–26.
7. Shen, Y. L., and N. A. Duffie (1993), "Comparison of Combinatorial Rules for Machine Error Budgets," *Annals of the CIRP*, Vol. 42 (1), pp. 619–621. 

Precision Grinding of Brittle Materials

Mark A. Piscotty, Kenneth L. Blaedel, Pete J. Davis, and Pete C. Dupuy

Manufacturing and Materials Engineering Division

Mechanical Engineering

High performance brittle materials, such as silicon, beryllium-oxide (BeO) and glasses, offer high-performance properties for demanding engineering applications. Similar to the need that motivated the development of diamond turning capabilities at Lawrence Livermore National Laboratory (LLNL), the demand for precision-machined brittle material components is driving the development of precision grinding. Precision grinding is often the only viable process to fabricate precision components in a cost-effective manner. The goal of our development project is to meet the needs of LLNL's programs for brittle material components that are difficult to manufacture. We focus on the process development and associated activities, such as process modeling, metrology and commercialization for medium- to high-volume production.

Introduction

For LLNL to meet the increasing demands of its programs, it is crucial that we extend our expertise in precision grinding.

The need for the development of cost-effective precision fabrication of brittle material components is driven by the increasing demand for high-performance components from LLNL's large programs, such as Weapons and Lasers. High-performance brittle materials such as silicon, glasses and a wide variety of ceramics will play an ever-increasing role in many of LLNL's and DOE's major programs. This project focuses on the precision grinding of BeO ceramic components to be used as heatsinks for mounted electrical components (**Fig. 1**). BeO is the preferred material for this application and others because of its rare combination of high thermal conductivity (~56% that of copper) and its low electrical conductivity. The challenge is developing a process to machine necessary heatsink features in BeO substrates while meeting optically-driven tolerance specifications.

Along with the need to develop precision fabrication and process techniques, computer modeling and other analytical capabilities are instrumental as tools to predict grinding wheel wear rates, material grindability and resultant characteristics of the workpiece. In addition, metrology processes are

required to provide process information feedback and to ensure the workpieces meet specifications.

LLNL's precision grinding core technology development effort encompasses a number of related tasks, all of which play key roles in advancing precision machining of brittle materials for programmatic applications and give it great potential for successful commercialization with outside vendors.

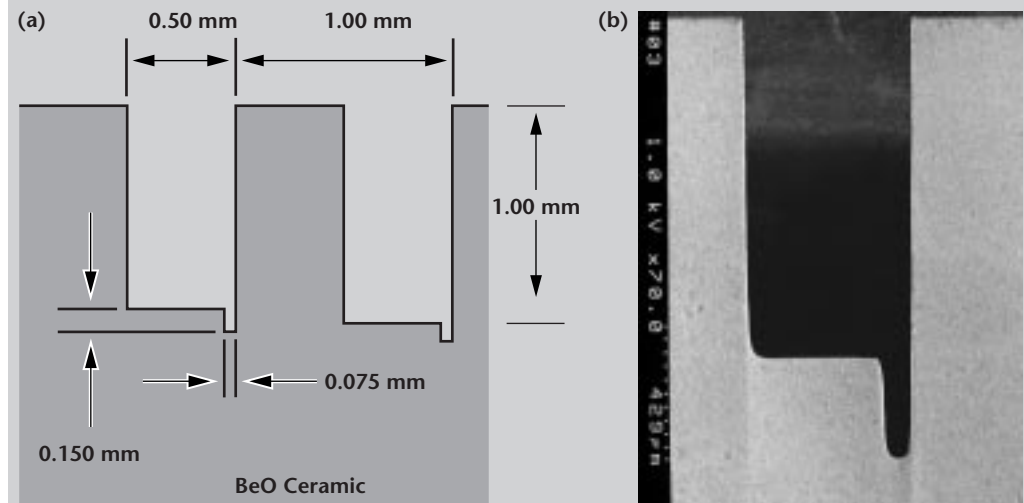
Progress

Precision grinding of brittle materials encompasses a variety of processes, including profile



Figure 1. BeO ceramic heatsink component.

Figure 2. (a) Typical heatsink dimensions; and (b) heatsink groove end view.



grinding, cylindrical grinding, and surface grinding.¹ In this project, the focus is profile grinding of intricate geometries in 2-mm-thick ceramic substrates. **Figure 2a** shows a schematic and dimensions of the experimental components used in this study.² Typical tolerances required for this component range from $\pm 1 \mu\text{m}$ to $\pm 5 \mu\text{m}$. An SEM end view of a precision ground sample feature is shown in **Fig. 2b**. Note that the internal corners display finite radii, which is an indication of corner wheel wear. Wheel wear is a major complicating factor in grinding small features such as these, since a small amount of wheel wear can result in out-of-specification workpieces.

In addition to the dimensions shown in **Fig. 2a**, other characteristics of the ground specimen also have stringent requirements. **Figures 3a** and **3b** show additional SEMs of a typical precision ground workpiece. The long vertical wall shown in **Fig. 3a** has both flatness and straightness tolerances of $\pm 1 \mu\text{m}$ along the groove length. Meeting these requirements entails stringent control of the side wheel wear and the ability to maintain the wheel in a free-cutting state. These two conditions are often adversarial because free-cutting wheels typically shed used diamond abrasives to expose sharp, fresh abrasives, which itself is a form of wheel wear. Excessive side wheel wear can produce canted vertical walls, resulting in unusable workpieces.

Brittle materials are highly susceptible to edge chipping during processes such as precision grinding. Zero-tolerance edge chipping is typically required as it can degrade the strength and performance of the component. **Figure 3b** shows an SEM used to examine the edges of a feature bottom for

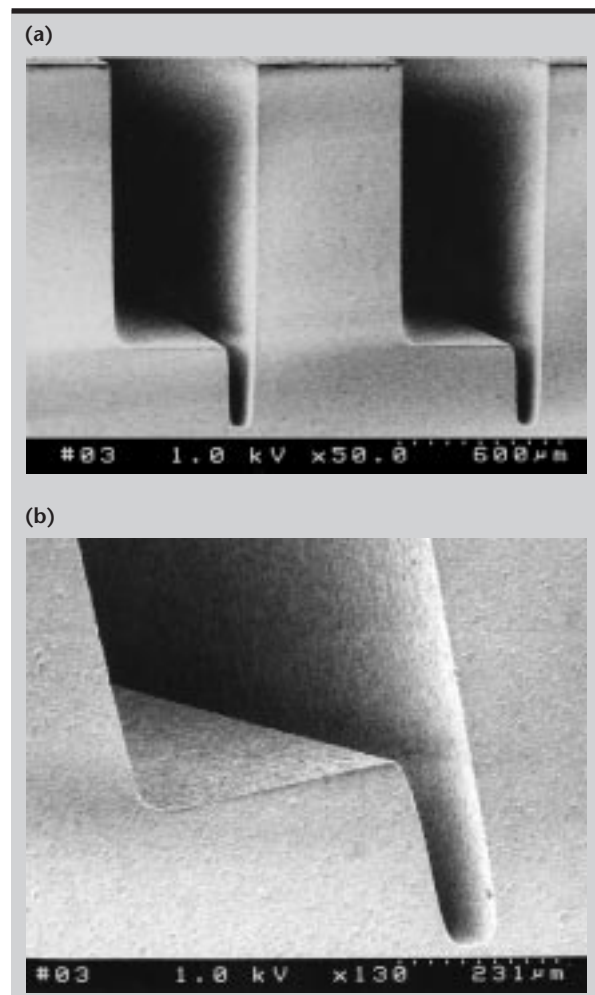


Figure 3. (a) SEM of heatsink features; and (b) SEM of feature bottom notch.

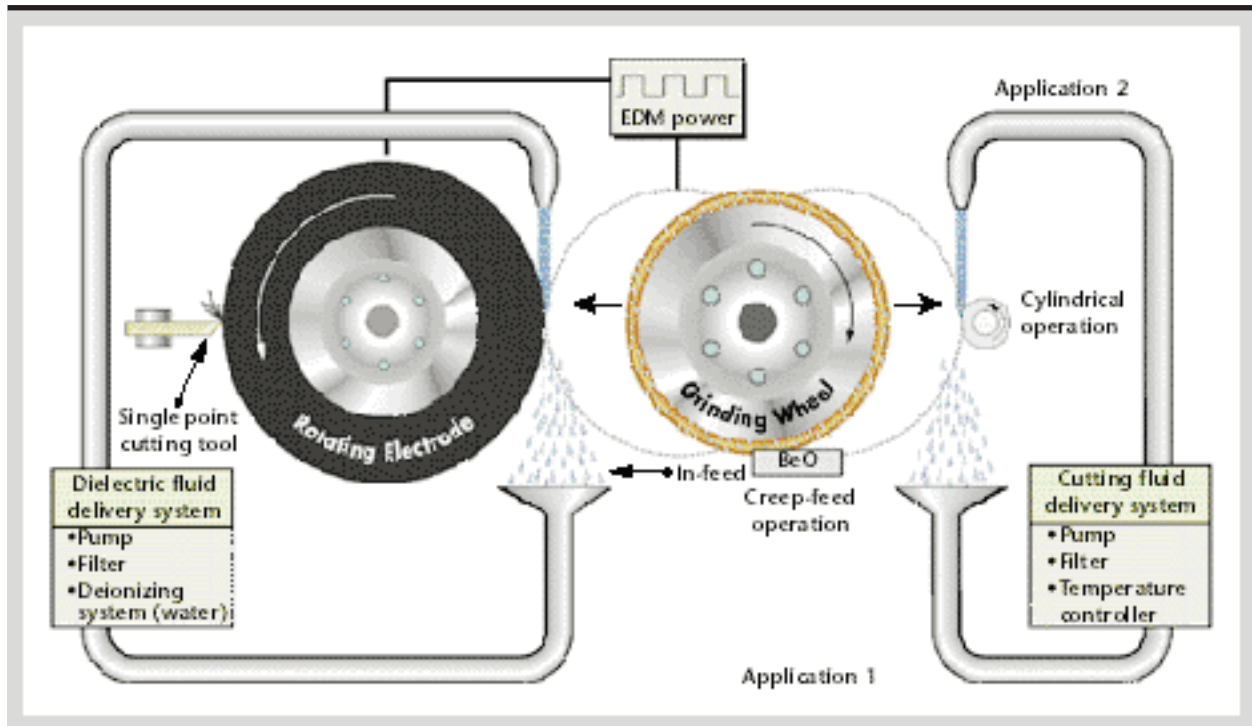


Figure 4. Schematic of machine tool set-up.

edge chipping. The nominal grain size of the BeO used in this study is 15 to 25 μm . To generate sharp corner surfaces without edge chipping requires that intragranular grinding take place. This requires that the grinding wheel maintain a well-dressed condition throughout the grinding cycle, ensured by intermittent dressing of the wheel during the grinding process.

A number of viable processes, each with its advantages and disadvantages, were possible candidates for machining these components. The process used at LLNL was selected because of its flexibility, robustness, and potential to be commercialized. Shown in the schematic in **Fig. 4** are two separate applications using the same basic process, one for creep feed grinding of flat substrates (BeO heatsinks) and the other cylindrical grinding (ceramic engine components).

An on-line electrical discharge machining (EDM) system is used to impart precision profiles on a metal bond, diamond abrasive grinding wheel. Features on the rotating graphite EDM electrode are turned on its outside diameter surface using a single point carbide tool and are used in the process to machine the profiles on the grinding wheel. In this case, a grinding wheel with two profiles is optimal, since two grinding passes are required to complete a groove. However, this process can be extended to generate additional profiles on a single grinding

wheel or to fabricate several profiled grinding wheels on a multiple wheel arbor. The ceramic workpieces are held in a chucking fixture below the profiled grinding wheel (**Fig. 5**).

Metrology

The unique heatsink configuration used in this project has several critical dimensions and requires geometric verification using off-line inspection procedures. These procedures involve a combination of both visual and contact metrology. Visual inspection is used for specific profile portions, such as the

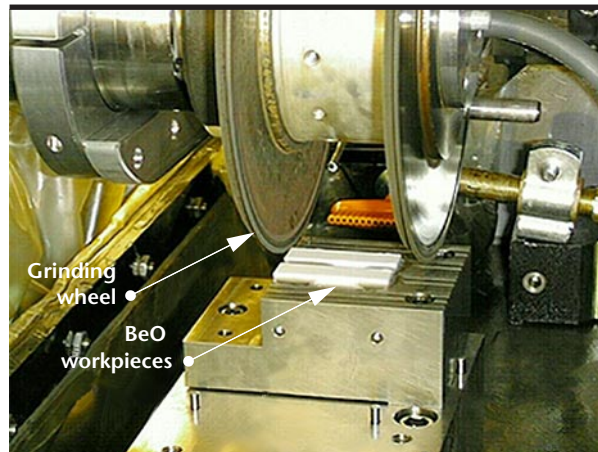


Figure 5. BeO heatsinks in grinding position.

flatness of the groove bottoms, the widths and depths of the relief notch at the bottom, and the flatness of the groove walls. Contact metrology is performed using a delicate stylus probe to allow interrogation of the grooves' inner geometries (walls and bottom).

Figures 6a and 6b show inspection photographs of the process using a precision coordinate measuring machine (CMM) located at Sandia National Laboratory in California. The touch probe is held in a low force sensor head, and axes-positioning feedback is provided from distance measuring laser interferometers. This inspection procedure enables each part to undergo 100% inspection, which is a valuable diagnostic during process development. As processes become more robust and proven, inspection procedures may be streamlined to increase throughput.

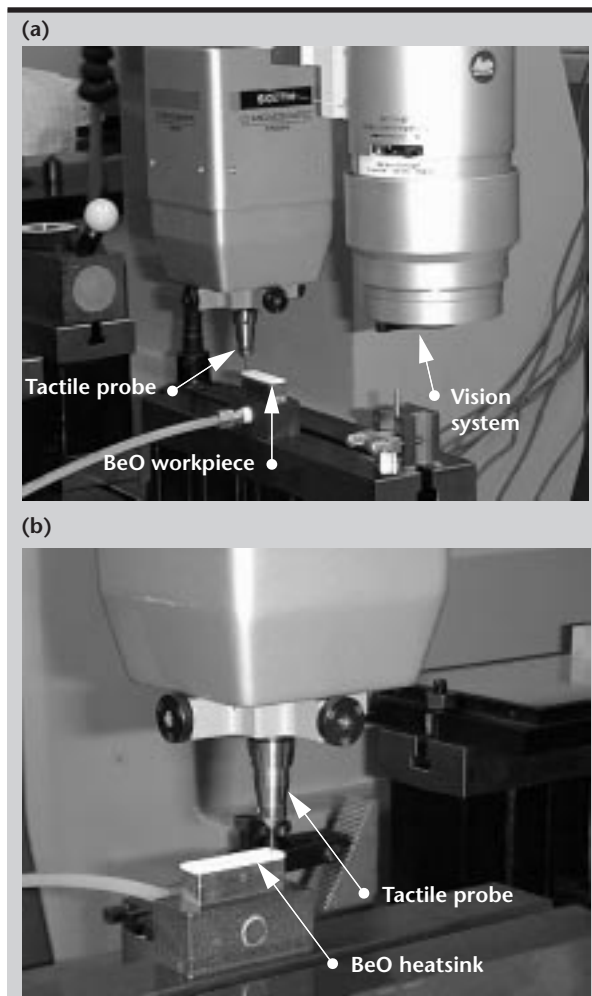


Figure 6. (a) Moore M48 CMM for heatsink metrology; and (b) set-up for tactile probe metrology.

Commercialization

While the primary goal of this project is to develop precision grinding, a secondary goal is to enable this technology to be commercialized with at least one outside vendor for higher volume and lower cost production for LLNL's programs.

A number of challenges were encountered during the effort to commercialize this technology. Among these challenges were determining technically competent vendors with the necessary machine tools for precision fabrication of ceramic components. In addition, the vendors must be willing and qualified to machine BeO, which is considered toxic in its powdered state. This narrowed the selection down to one vendor, Brush Wellman in Tucson, AZ. Brush Wellman is the sole supplier of BeO in the U.S. and has significant experience machining BeO for customers.

However, the precision needed to fabricate these heatsink components was beyond their experience and we therefore are working closely with them to transfer our process technology to them. Because Brush Wellman's machine tools and machining capabilities vary significantly from those at LLNL, we tailor the technology transfer to accommodate this.

Brush Wellman owns two machine tools that can meet the stringent performance criteria to fabricate BeO heatsinks in medium lot sizes (about 100 pieces per lot). The first is a surface grinder that has been used as a workhorse for other precision-ground BeO components. The second machine tool, which we feel has the most promise for delivering these heatsinks at the lowest cost, is an MT1612 precision slicing machine. This machine is capable of using a ganged wheel arbor (multiple wheels mounted on one precision arbor) and has three-axes-positioning accuracy of better than 1 μm . Collaborations between LLNL and Brush Wellman are establishing processes on both these machine tools at Brush Wellman, now the vendor of choice for these heatsinks.

Modeling

The modeling development of this project centers on understanding the mechanisms for generating and propagating sub-surface damage (SSD) during the precision grinding of brittle materials. This has been studied by a number of researchers using a variety of models and techniques.^{3,4,5} The modeling technique investigated involves a continuum damage mechanics (CDM) model developed at the University of Connecticut under Professor B. Zhang and Ph.D.

candidate R. Monahan. The current CDM model investigates the resulting SSD generated by a single grit material removal.

While this model has interesting implications and information, a new model will include material removal interaction among several grits in a grinding wheel, which is more characteristic of a real grinding process. The CDM model introduces inelasticity and damage to accommodate the non-linear responses of brittle materials. The current states of effective stress and damage and hydrostatic stress are used to simulate the cumulative anisotropic damage of the brittle material. The next generation of this model will be developed at the University of Connecticut with input and review from LLNL.

Conclusions

Precision fabrication of programmatically important brittle material components is a vital capability that is being maintained and extended at LLNL. Precision grinding of brittle materials is often the procedure of choice for this type of fabrication, since it offers many advantages over other possible methods. This project leveraged a number of these advantages including process flexibility, readily available precision grinding machine tools and components, beneficial ties to industrial processes and vendors, and the ability to transfer a precision process to a vendor for large volume commercialization.

Future Work

Clearly, grinding has a long history and recent developments in the area of precision grinding are producing remarkable results. However, precision grinding of brittle materials remains a relatively young technology area compared to other techniques such as diamond turning, and thus cries out for more research.

Future work should be focused on understanding the fundamentals of the material removal mechanisms, wheel wear phenomenon, the dynamics of the precision grinding process, and the propagation of surface and subsurface damage in the workpieces. Understanding the implications of how these mechanisms affect the precision of ground brittle material components is key to realizing the full potential of this fabrication process.

Semiconductor materials, thin films and optical systems are in the forefront of advanced materials that play a critical role in many LLNL programs.

New coating and fabrication techniques are producing materials to meet the ever-increasingly stringent dimensional, defect and SSD requirements. To use these materials to their maximum potential, their dimensions and defect state must be measured with heretofore-unattainable precision.

Conventional SSD measurement techniques typically focus on destructive methods, including taper polishing and tunneling electron microscopy.^{6,7} X-ray diffraction has been used with little success since it works best with well-defined crystalline substrates.

It became obvious during the course of this project that the technology to quantitatively evaluate SSD in a nondestructive manner demands substantial research and development. An *in-situ*, nondestructive evaluation technique would be an extremely valuable and unique tool for interrogating SSD as a result of grinding, lapping and polishing.

Current methods to quantitatively evaluate SSD are labor- and time-intensive, and destroy the surface of the workpiece being evaluated. Drs. S. Soares (California Institute of Technology) and B. Zhang have developed a proposal for a nondestructive method to evaluate SSD in brittle materials.

References

1. Komanduri, R., D. A. Lucca, and Y. Tani (1997), "Technological Advances in Fine Abrasive Processes," *Annals of CIRP*, **46**, pp. 1-52.
2. Drawing No. AAA98-107146-OA, Lawrence Livermore National Laboratory, Livermore, California.
3. Fahrenthold, E. P. (1991), "A Continuum Damage Model for Fracture of Brittle Solids Under Dynamic Loading," *Journal of Applied Mechanics*, **58**(4), pp. 904-909.
4. Hu, K. X., and A. Chandra (1993), "A Fracture Mechanics Approach to Modeling Strength Degradation in Ceramic Grinding Process," *Journal of Engineering for Industry*, **115**(1), pp. 73-84.
5. Ju, J. W., and X. Lee (1991), "Micromechanical Damage Models for Brittle Solids, I: Tensile Loadings," *Journal of Engineering Mechanics*, **117**(7), pp. 1495-1536.
6. Zhang, B. (1995), "Subsurface Evaluation of Ground Ceramics," *Annals of CIRP*, **44**, pp. 263-266.
7. Xu, H. K. (1996), "Material Removal and Damage Formation Mechanisms in Grinding Silicon Nitride," *Journal of Material Research*, **11**(7). 